ELECTRIC SAIL FOR NEAR-EARTH ASTEROID SAMPLE RETURN MISSION: CASE 1998 KY26

Alessandro A. Quarta,[1]

Giovanni Mengali, [2]

and

Pekka Janhunen [3]

Abstract

The electric solar wind sail (E-sail) is an innovative propellantless concept for interplanetary space propulsion that uses the natural solar wind as a thrust source with the help of long, artificially charged tethers. The characteristic property of an E-sail based spacecraft is that the propulsive acceleration scales as the inverse Sun-spacecraft distance, and the thrust vector can be varied within about 30 degrees away from radial direction.

The aim of this paper is to estimate the transfer times required to fulfill a mission toward the near-Earth asteroid 1998 KY26. In doing so the propulsive acceleration of the E-sail, at a reference distance from the Sun, is used as a performance parameter so that the numerical results are applicable to E-sails of different sizes and different payload masses. The paper shows that the flight time scales nearly linearly with the inverse of the spacecraft maximum propulsive acceleration at 1 Astronomical Unit from the Sun, when the acceleration is greater than $0.3\,\mathrm{mm/s^2}$. For smaller propulsive accelerations the relationship for the flight time is more involved, because the transfer trajectory is complex and more than one revolution around the Sun is necessary to accomplish the mission. The numerical analysis involves a sample return mission in which the total flight time is parametrically correlated with the

[1]Department of Aerospace Engineering, University of Pisa, I-56122, Pisa, Italy, E-mail: a.quarta@ing.unipi.it

[2]Department of Aerospace Engineering, University of Pisa, I-56122, Pisa, Italy, E-mail: g.mengali@ing.unipi.it

[3]Finnish Meteorological Institute, FIN-00101 Helsinki, Finland, E-mail: pekka.janhunen@fmi.fi

starting date for a given E-sail propulsion system.

Keywords: Electric sail, near-Earth asteroid exploration, mission analysis.

NOMENCLATURE

$\mathbb{A}$	=	matrix $\in \mathbb{R}^{6\times 3}$, see Eq. (7)
$\boldsymbol{a}$	=	spacecraft propulsive acceleration
$a_\oplus$	=	spacecraft characteristic acceleration
$\boldsymbol{d}$	=	vector $\in \mathbb{R}^{6\times 1}$, see Eq. (8)
e	=	orbital eccentricity
f, g, h, k	=	modified equinoctial elements
H	=	Hamiltonian function
i	=	orbital inclination
J	=	performance index
L	=	true longitude
p	=	semilatus rectum
r	=	Sun-spacecraft distance, with $r_\oplus \triangleq 1\,\mathrm{AU}$
$\boldsymbol{r}$	=	spacecraft position vector
t	=	time
$\boldsymbol{x}$	=	state vector
α	=	sail cone angle
Δt	=	flight time
$\boldsymbol{\lambda}$	=	adjoint vector
λ	=	adjoint variable
$\mu_\odot$	=	Sun's gravitational parameter
ν	=	true anomaly
τ	=	switching parameter
Ω	=	right ascension of the ascending node

ω	=	argument of perihelion

Subscripts

AE	=	asteroid-Earth phase
EA	=	Earth-asteroid phase
f	=	final
i	=	initial
max	=	maximum
w	=	waiting phase
$\odot$	=	Sun

Superscripts

$\wedge$	=	unit vector
(ss)	=	photonic solar sail

INTRODUCTION

The successful conclusion of Japanese Hayabusa mission, which, on 13 June 2010, returned to Earth with a material sample from asteroid 25143 Itokawa (Baker 2006), has renewed the scientific community's interest in studying those minor celestial bodies that populate the interplanetary space surrounding Earth. Unlike previous missions, such as Galileo, which first obtained close images of asteroids Ida and Gaspra during its flight towards Jupiter, or NASA's probe Near Earth Asteroid Rendezvous (NEAR) Shoemaker, which on 2001 touched down on asteroid 433 Eros, the Hayabusa mission has first demonstrated the technical feasibility of retrieving material samples from a near-Earth asteroid (Barucci et al. 2011). This new frontier will be further advanced by Origins-Spectral Interpretation-Resource Identification-Security-Regolith Explorer (OSIRIS-REx) mission, whose launch is scheduled for 2016, and whose aim is to reach the potentially hazardous asteroid 1999 RQ36 in 2019.

From a commercial viewpoint, returning an asteroid sample to the Earth is only the first step toward a future exploitation of resources from celestial bodies (Lewis 1996). In fact, asteroids contain materials that could be used for different purposes both in space and on Earth (Metzger et al. 2012). In scientific terms, an in-depth analysis of asteroid samples would guarantee a substantial knowledge improvement about the Solar System evolution (Barucci et al. 2011). In particular, a collection of samples with chemically unbound water from near Earth asteroids would represent a concrete step forward in understanding water distribution within interplanetary space, including the question from where Earth received its water. A main objective of OSIRIS-REx mission is, in fact, to return an asteroid sample to Earth, in order to reveal the presence of volatiles and organics that could represent the starting material for chemical evolution.

Within the set of asteroids that are accessible to spacecraft rendezvous, asteroid 1998 KY26 has interesting characteristics. It was discovered in 1998 when it passed at 2.1 lunar distances from Earth (Ostro et al. 1999). It is a small asteroid of only 30 m diameter and, according to a spectral analysis, it is a carbonaceous body (C-type asteroid). Therefore, it is likely to contain water. Unfortunately, its fast rotation speed (about 0.11 rpm) poses severe constraints against the possibility of mining it to collect material samples. Nevertheless, the 1998 KY26 is chosen in this paper as a representative near-Earth asteroid candidate target for the preliminary design of a sample return mission for a spacecraft, whose primary propulsion system is an electric solar wind sail (E-sail).

The E-sail, see Fig. 1, is an innovative deep space propulsion concept that uses the solar wind dynamic pressure for generating thrust without the need of reaction mass (Janhunen 2010; Janhunen 2009; Janhunen et al. 2010). A spacecraft with an E-sail propulsion system, is spun around its symmetry axis and uses the centrifugal force to deploy and stretch out a number of thin, long and conducting tethers, which are kept in a high positive potential by an onboard electron gun (Janhunen et al. 2010). The latter compensates the electron current gathered by the conducting tethers from the surrounding solar wind plasma.

Between the spacecraft and each of the tethers there is a potentiometer that allows each tether to be in a slightly different potential from the others. Because the thrust magnitude depends on the tether potential, this gives a way to control the thrust experienced by each tether individually and guarantees the possibility of attitude control of the tethers spin-plane. In fact the spin-plane can be turned by modulating the potentiometer settings by a sinusoidal signal synchronized to the rotation. The phase of the signal determines the direction in which the spin-plane turns and its amplitude regulates how fast such a turning occurs.

Under mild assumptions (Janhunen et al. 2010), a characteristic feature of an E-sail propulsion system is that the thrust produced is proportional to $1/r$, where r is the Sun-spacecraft distance. More precisely, such a thrust variation with the solar distance is valid provided that the potential sheath overlapping between different tethers is negligible, that the available electric power varies as $1/r^2$, and that the employed tether voltage is independent of r. However, the thrust vector control capability of an E-sail based spacecraft is moderate, because the thrust direction can be changed by inclining the spin-plane with respect to the solar wind flux (which is nearly coincident with the radial direction) within a cone whose half-width is around 30 deg. This peculiarity poses a challenge in mission analysis from the viewpoint of trajectory design, especially when a rendezvous-mission is considered.

MISSION ANALYSIS

The asteroid sample return mission is analyzed in an optimal framework (from the viewpoint of the flight time) as a function of the spacecraft characteristic acceleration $a_\oplus$, that is, the maximum propulsive acceleration at a reference distance $r_\oplus \triangleq 1\,\mathrm{AU}$ from the Sun. The E-sail based spacecraft is modeled as a point-mass vehicle with a constant mass and a propulsive acceleration $\boldsymbol{a}$ given by

$$\boldsymbol{a} = a_\oplus \, \tau \left(\frac{r_\oplus}{r}\right) \hat{\boldsymbol{a}} \qquad \text{with} \qquad \arccos(\hat{\boldsymbol{a}} \cdot \hat{\boldsymbol{r}}) \triangleq \alpha \leq \alpha_{\max} \tag{1}$$

where the hat symbol denotes a unit vector, while the switching parameter $\tau = (0, 1)$ is a dimensionless coefficient that models the E-sail on/off condition and is introduced to account for coasting arcs in the interplanetary trajectory. In particular, the spacecraft propulsive thrust can be turned off ($\tau = 0$) at any time by simply switching off the onboard electron gun. The sail cone angle α, that is, the angle between $\hat{\boldsymbol{a}}$ and $\hat{\boldsymbol{r}}$, is assumed to have an upper bound of $\alpha_{\max} \triangleq 30\,\text{deg}$. As a result, the propulsive thrust vector lies within a conical region whose axis coincides with the Sun-spacecraft direction, see Fig. 2. Indeed (Janhunen et al. 2007), only the component of the solar wind perpendicular to the tethers produces a propulsive thrust, while the flow parallel to the tethers has no effect. As a result, a simple geometrical consideration shows that for a set of spinning tethers inclined at an angle θ with respect to the solar wind flow, the net thrust is directed at an angle $\alpha \simeq \theta/2$. Cone angles larger than about 30 deg are likely to be impractical because of the thrust reduction at high values of α and, possibly, due to mechanical instabilities.

The heliocentric orbital parameters of Earth and asteroid 1998 KY26 are taken from JPL ephemerides (Standish 1998; Standish 1990) and are summarized in Table 1. All simulations have been performed assuming a direct transfer (that is, without gravity assist maneuvers) between the two celestial bodies. Also, the optimal transfer trajectory was found under the assumption of a spacecraft deployment on a parabolic Earth escape trajectory, that is, with zero hyperbolic excess with respect to the starting planet. This is a conservative hypothesis in terms of mission transfer time. Also note that the effect of a hyperbolic excess energy different from zero can be taken into account in the optimization process only provided that the characteristics of the launch system are given.

The whole space mission can be ideally divided into three phases, as is schematically shown in Fig. 3. In a first transfer phase, whose time length is Δt_{EA}, the spacecraft is transferred from the Earth's heliocentric orbit to the asteroid's orbit. At the end of this phase the spacecraft concludes its rendezvous maneuver with the target asteroid and maintains a prescribed orbit relative to it. In the second phase, referred to as scientific phase, the spacecraft completes the prescribed scientific measurements. The time interval of this second phase is Δt_w (waiting time). In this phase a lander can be used to possibly reach the asteroid's surface and collect material samples. At the end of the second phase the lander (or part of it) performs a docking maneuver with the E-sail based spacecraft. The third phase starts at the docking instant and ends with an Earth's rendezvous (with no hyperbolic excess), within a time interval of Δt_{AE}. According to this simplified model the total mission time Δt is

$$\Delta t = \Delta t_{\mathrm{EA}} + \Delta t_w + \Delta t_{\mathrm{AE}}. \tag{2}$$

For a given value of spacecraft characteristic acceleration $a_\oplus$, the flight times for the first and last mission phases have been calculated by minimizing the time interval required for the rendezvous-maneuvers (Earth-asteroid and asteroid-Earth phases). Accordingly, the two values $\Delta t_{\mathrm{EA}}(a_\oplus)$ and $\Delta t_{\mathrm{AE}}(a_\oplus)$ have been calculated numerically as a function of the starting date of each phase in terms of Modified Julian Date (MJD). The mathematical model used in the trajectory optimization has been summarized in the appendix. Note that the optimization algorithm is fully general, and can be applied, with minor changes, to a wide range of mission scenarios. Due to numerical challenges and the number of required iterations involved in solving this kind of problem, the solution has been obtained through a two-step procedure, which is now described in detail.

Orbit-to-orbit optimal trajectories

Firstly (step one), minimum time, three-dimensional transfer trajectories have been calculated, for phases one and three, by neglecting any ephemeris constraint on the two celestial bodies. In other terms, within an orbit-to-orbit optimal trajectory, the spacecraft matches the (Keplerian) heliocentric orbit of the two celestial bodies at both departure and arrival time instants. This implies that only the shape and orientation of the two orbits (corresponding to the data of Table 1) were taken into account in the optimization process, see the appendix. The numerical procedures used here have been validated in previous studies (Mengali et al. 2008; Quarta and Mengali 2010). The main information that can be obtained from this analysis is the optimal performance (that is, the minimum flight time) during a single phase as a function of the spacecraft characteristic acceleration only and a rough estimation of the launch window within which the optimal transfer can take place.

To obtain a cost estimate of phases one and three, observe that each phase, in a two-impulse mission scenario, requires a total minimum velocity variation of about 3.4 km/s, that is, a velocity variation of 2.895 km/s at Earth's orbit, and a velocity variation of 0.505 km/s at asteroid's orbit. Therefore, a four-impulse sample return mission with a three phases scenario, see Fig. 3, requires at least a total velocity variation of about 6.8 km/s $= 2 \times$ 3.4 km/s. Note that, according to the rocket equation, a velocity variation of 6.8 km/s corresponds to a propellant mass fraction of about 86.2% when a (conservative) specific impulse of 350 s is assumed. Within an optimal two-impulses scenario (for phases one and three), the Keplerian transfer trajectory, see Fig. 4, is characterized by a semimajor axis of 1.248 AU, an eccentricity of 0.1858, an inclination of 0.6523 deg, a longitude of ascending node of 113.36 deg, and an argument of periapsis of 182.92 deg.

Of course, a velocity variation less than 3.4 km/s (for phases one and three) could be potentially obtained using a multiple-impulse transfer trajectory. In that case the total mission's cost should be evaluated, in an optimal framework, by minimizing the sum of the velocity variations for each impulse. However, such an analysis is beyond the aim of this paper.

The main results concerning the first mission phase have been summarized in Table 2, while Table 3 shows the corresponding results for the third (return) phase. The variable ν_i (or ν_f) represents the spacecraft heliocentric true anomaly along the starting (arrival) orbit at the initial (final) time instant. Recall that the spacecraft's starting and arrival orbit coincides with the heliocentric (Keplerian) orbit of one of the two celestial bodies of the problem. The fifth column of Tables 2 and 3 shows the number of complete revolutions around the Sun during the mission phase.

Tables 2 and 3 clearly show a rapid increase in the flight time by decreasing the spacecraft characteristic acceleration $a_\oplus$. The simulation results can be fitted by closed-form expressions that are useful for preliminary mission analysis. For example, flight time and spacecraft characteristic acceleration are related by the following best-fit curve

$$\Delta t_{\mathrm{EA}} \simeq 83.82\, a_\oplus^{-1.201} \tag{3}$$

$$\Delta t_{\mathrm{AE}} \simeq 83.39\, a_\oplus^{-1.214} \tag{4}$$

where $a_\oplus \in [0.1,\, 1]\,\mathrm{mm/s^2}$ and the flight time is expressed in days.

From Table 2 a rapid transfer to the asteroid 1998 KY26, that is, a mission whose transfer time is less than one terrestrial year (Mengali and Quarta 2009), requires a characteristic acceleration $a_\oplus \geq 0.3\,\mathrm{mm/s^2}$. In this case, the mission is completed within less than a full revolution about the Sun, see Fig. 5, as is indicated by the fifth column of Table 2. Instead, if $a_\oplus < 0.3\,\mathrm{mm/s^2}$, the heliocentric trajectory is more involved, with multiple revolutions around the Sun, see Fig. 5, and the flight time increases up to exceeding four years if $a_\oplus < 0.09\,\mathrm{mm/s^2}$, see Table 2.

A similar result holds for the return phase, and Fig. 6 shows a spacecraft trajectory projection on the ecliptic plane.

To better emphasize the capability of performing such a mission type, the performance of an E-sail are now compared to those of an ideal (photonic) solar sail. The latter may be thought of as being equivalent to a perfectly reflecting flat surface. The propulsive acceleration $\boldsymbol{a}^{(ss)}$ provided by an ideal solar sail may be expressed as

$$\boldsymbol{a}^{(ss)} = a_{\oplus}^{(ss)} \left(\frac{r_\oplus}{r}\right)^2 \cos^2 \alpha^{(ss)}\, \hat{\boldsymbol{a}}^{(ss)} \tag{5}$$

where $\hat{\boldsymbol{a}}^{(ss)} \triangleq \boldsymbol{a}^{(ss)}/\|\boldsymbol{a}^{(ss)}\|$, and $\alpha^{(ss)} \in [0,\, \pi/2]$ is the solar sail cone angle, that is, the angle between the direction of $\hat{\boldsymbol{a}}^{(ss)}$ and that of the incoming photons. In an ideal solar sail the propulsive acceleration unit vector $\hat{\boldsymbol{a}}^{(ss)}$ coincides with the unit vector normal to the sail nominal plane in the thrust direction.

In Eq. (5), $a_{\oplus}^{(ss)}$ is the spacecraft characteristic acceleration, that is, the maximum propulsive acceleration at a distance equal to 1 AU from the Sun. Note that, unlike an E-sail, the maximum modulus of the solar sail propulsive acceleration varies as the inverse square distance from the Sun. Also, the solar sail cone angle $\alpha^{(ss)}$ is only constrained by the condition that the propulsive acceleration cannot by oriented toward the Sun.

Even though an E-sail and a solar sail are both propellantless propulsion systems, these two systems are much different in terms of dimensions, required mass and also from the viewpoint of the physical mechanism through which the thrust is produced. Therefore, a comparison between the two propulsion systems must be performed with care and taking into account not only the flight time, but also other quantities such as the characteristic dimensions of the two systems and the allowable payload mass fraction.

It will be now emphasized that, within the mission scenario discussed in this paper, an E-sail offers better performance than an ideal solar sail. To prove this claim, a comparison between the two propellantless propulsion systems is made under suitable assumptions. The mission consists of an orbit-to-orbit transfer in which Earth-asteroid and asteroid-Earth transfer phases are both analyzed. Assuming a flight time corresponding to the value necessary for an E-sail to complete the mission, it is possible to calculate the minimum characteristic acceleration $a_{\oplus}^{(ss)}$ required by a solar sail to fulfill the same mission. The optimization model necessary to solve such a problem has been adapted from Mengali and Quarta (2009), to which the interested reader is referred for an in depth discussion. The numerical simulations results are summarized in the last column of Tables 2 and 3.

Note that, the flight time being the same, the characteristic acceleration required by a solar sail is greater than that corresponding to an E-sail, that is, $a_{\oplus}^{(ss)} > a_{\oplus}$. This implies that, from the viewpoint of the combination flight time-characteristic acceleration and for this particular mission scenario, an E-sail offers better performance than a solar sail. The reason of this result is closely related to the type of optimal trajectory obtained to fulfill the mission. Indeed, as is illustrated in Fig. 4, the heliocentric orbit of asteroid 1998 KY26 has a perihelion radius close to 1 AU (exactly equal to 0.9838 AU). Because the heliocentric orbit of Earth is nearly circular with a radius equal to 1 AU, it can be verified that the transfer trajectories for both an E-sail and a solar sail take place at a solar distance greater than 1 AU. Under these conditions, as stated, an E-sail behaves better than a solar sail from the point of view of the propulsive acceleration's maximum modulus.

Rendezvous constrained transfers

The actual position of the two celestial bodies along their orbits must now be taken into account (second step of the procedure). The angular position of both Earth and target asteroid is obtained, in a simplified way, using a two-body dynamical model and the data of Table 1.

For a given value of the spacecraft characteristic acceleration and a time interval within which the mission must be fulfilled, it is possible to look for the best available launch window using the orbit-to-orbit optimal results from the previous section. In this study, a spacecraft characteristic acceleration $a_{\oplus} = 0.1\,\mathrm{mm/s^2}$ and a time interval of ten years from January 1, 2020 will be assumed. The optimal launch window opens on August 2026 (MJD = 61254), when the transfer time is $\Delta t_{\mathrm{EA}} \simeq 1349\,\mathrm{days}$ (this length is close to the orbit-to-orbit reference value of Table 2).

Note that a characteristic acceleration of $0.1\,\mathrm{mm/s^2}$ is expected to be a rather conservative value, which should be guaranteed by a full scale E-sail of the first generation. Also, current estimates induce to think that such a value could be improved of an order of magnitude for an E-sail of the second generation. As such, a characteristic acceleration of about $1\,\mathrm{mm/s^2}$ should be a reasonable value for a near term E-sail.

Having found an optimal solution with a planetary ephemerides constraint, the launch date was modified to get parametric relationships between mission starting date and flight time Δt_{EA}. The results of this analysis are summarized in Fig. 7. The figure shows a marked dependence of the flight time on the start date and the existence of a second (sub-optimal) launch window on June 2023 (MJD = 60098), with a corresponding flight time of about 100 days longer than the optimal value.

The asteroid-Earth return phase was then investigated assuming a tentative waiting time Δt_w of one year. A parametric study concerning the return phase involves the time Δt_{AE} as a function of the reentry date within the interval January 2028 – January 2033. The results of this numerical analysis are summarized in Fig. 8. In particular, Fig. 8 shows a sub-optimal launch date in October 2029 (MJD = 62420) with a flight time of about 1390 days. Such a result is not consistent with the optimal transfer of the first phase unless the starting launch window is moved earlier (with a consequent increase in the Earth-asteroid transfer time). This suggests calculating the end mission date as a function of the starting date and the waiting time by suitably combining the information from Figs. 7 and 8.

The results of this analysis have been summarized in Fig. 9, which shows the mission end date as a function of the launch window for different values of waiting time ($\Delta t_w = \{0, 0.5, 1, 1.5, 2\}$ years). Note that $\Delta t_w = 0$ corresponds to the limiting case in which the spacecraft performs an asteroid rendezvous and immediately starts the returning flight to Earth. A more interesting mission scenario is obtained when the spacecraft waits around the asteroid for a time interval sufficient to mine the asteroid's surface and collect the material samples. In this case, assuming $a_\oplus = 0.1\,\mathrm{mm/s^2}$ and a waiting time of about one year, Fig. 9 shows that the whole mission can be fulfilled in slightly less than 11 years.

CONCLUSIONS

Even though the E-sail propulsion system is expected to enable high characteristic accelerations with small and moderate payloads, in an asteroid sample return scenario or in a mission application that involves a large scientific payload, a small spacecraft characteristic acceleration is also of practical interest. The asteroid 1998 KY26 has been chosen in this study as a significant candidate for a possible E-sail based mission. The main results of this paper are contained in Tables 2 and 3 where the E-sail flight time to and from the near-Earth asteroid 1998 KY26 are given, parameterized by the characteristic acceleration $a_\oplus$, which is determined by the payload mass relative to the E-sail size. A mission scenario that considers the ephemeris constraints, shows that an E-sail with a characteristic acceleration of $0.1\,\mathrm{mm/s^2}$ (a rather low value for a sail of the next generation) is able to complete a sample return mission, with a waiting time of one year, in about 11 years. Moreover the E-sail offers an interesting flexibility in the launch window. Indeed, the propulsion system's continuous thrust could be used to maintain the same Earth-return date by changing both the transfer time and the waiting time.

A final remark concerns the feasibility of further reducing the mission time. A lunar gravity assist maneuver can be used to obtain (or damp) a moderate hyperbolic excess speed when leaving or entering the Earth's trajectory. That happens, of course, at the cost of introducing further restrictions on the launch window. In particular, when returning to Earth, if the target is to bring the payload to ground, it is often acceptable to leave it on collision course with Earth with a nonzero hyperbolic excess speed. This last option will imply a reduction of travel time. In this sense the mission times calculated in this paper are conservative estimates.

ACKNOWLEDGMENTS

This research was financed within the European Community's Seventh Framework Programme ([FP7/2007-2013]) under grant agreement number 262733 and the Academy of Finland grant decision 250591.

APPENDIX: E-SAIL TRAJECTORY OPTIMIZATION

The equations of motion of an E-sail based spacecraft are written in terms of non-singular parameters as the Modified Equinoctial Orbital Elements (Walker et al. 1985; Walker 1986) (MEOE) p, f, g, h, k, and L. Accordingly, within a heliocentric inertial reference frame, the E-sail dynamics is described by the following first-order vectorial differential equation (Betts 2000):

$$\dot{\boldsymbol{x}} = a_\oplus \, \tau \left(\frac{r_\oplus}{r}\right) \mathbb{A} \, \hat{\boldsymbol{a}} + \boldsymbol{d} \tag{6}$$

where $\boldsymbol{x} \triangleq [p,\, f,\, g,\, h,\, k,\, L]^{\mathrm{T}}$ is the state vector of the problem, and $\hat{\boldsymbol{a}}$ is the propulsive acceleration unit vector whose components should be expressed in a local-vertical/local-horizontal orbital reference frame, see also Eq. (1). In Eq. (6), $\mathbb{A} \in \mathbb{R}^{6\times 3}$ is a matrix in the form:

$$\mathbb{A} \triangleq \sqrt{\frac{p}{\mu_\odot}} \begin{bmatrix} 0 & \left[\dfrac{2\,p}{1+f\,\cos L + g\,\sin L}\right] & 0 \\ [\sin L] & \left[\dfrac{(2+f\,\cos L+g\,\sin L)\,\cos L + f}{1+f\,\cos L+g\,\sin L}\right] & \left[-\dfrac{g\,(h\,\sin L - k\,\cos L)}{1+f\,\cos L+g\,\sin L}\right] \\ [-\cos L] & \left[\dfrac{(2+f\,\cos L+g\,\sin L)\,\sin L + g}{1+f\,\cos L+g\,\sin L}\right] & \left[\dfrac{f\,(h\,\sin L - k\,\cos L)}{1+f\,\cos L+g\,\sin L}\right] \\ 0 & 0 & \left[\dfrac{\left(1+h^2+k^2\right)\,\cos L}{2\,(1+f\,\cos L+g\,\sin L)}\right] \\ 0 & 0 & \left[\dfrac{\left(1+h^2+k^2\right)\,\sin L}{2\,(1+f\,\cos L+g\,\sin L)}\right] \\ 0 & 0 & \left[\dfrac{h\,\sin L - k\,\cos L}{1+f\,\cos L+g\,\sin L}\right] \end{bmatrix} \tag{7}$$

where $\mu_\odot \triangleq 132\,712\,439\,935.5\,\mathrm{km^3/s^2}$ is the Sun's gravitational parameter, and the vector $\boldsymbol{d} \in \mathbb{R}^{6\times 1}$ is defined as

$$\boldsymbol{d} \triangleq \left[0,\, 0,\, 0,\, 0,\, 0,\, \sqrt{\mu_\odot\, p}\, \left(\frac{1+f\,\cos L+g\,\sin L}{p}\right)^2\right]^{\mathrm{T}} \tag{8}$$

Note that p is the semilatus rectum of the spacecraft osculating orbit, whereas the transformations from MEOE to the classical orbital elements are given by

$$a = \frac{p}{1 - f^2 - g^2} \tag{9}$$

$$e = \sqrt{f^2 + g^2} \tag{10}$$

$$i = 2 \ \arctan \sqrt{h^2 + k^2} \tag{11}$$

$$\sin \omega = g\, h - f\, k \quad , \quad \cos \omega = f\, h + g\, k \tag{12}$$

$$\sin \Omega = k \quad , \quad \cos \Omega = h \tag{13}$$

$$\nu = L - \Omega - \omega \tag{14}$$

where a is the semimajor axis, e is the eccentricity, i the orbital inclination, ω is the argument of perihelion, Ω is the longitude of the ascending node, and ν is the true anomaly of the spacecraft's osculating orbit. On the other hand, the transformations from classical orbital elements to MEOE are

$$p = a \, \left(1 - e^2\right) \tag{15}$$

$$f = e \, \cos\left(\omega + \Omega\right) \tag{16}$$

$$g = e \, \sin\left(\omega + \Omega\right) \tag{17}$$

$$h = \tan(i/2) \, \cos \Omega \tag{18}$$

$$k = \tan(i/2) \, \sin \Omega \tag{19}$$

$$L = \Omega + \omega + \nu \tag{20}$$

In Eq. (6), the Sun-spacecraft distance r may be expressed as a function of MEOE as (Betts 2000)

$$r = \frac{p}{1 + f\,\cos L + g\,\sin L} \tag{21}$$

Consider the first phase of the sample return mission, that is, the Earth-asteroid phase (the same method can be easily extended to the last phase, or the asteroid-Earth phase). Assuming, as previously stated, a zero hyperbolic excess with respect to the starting planet, the initial spacecraft osculating orbit coincides with the Earth's (Keplerian) heliocentric orbit. Table 1 summarizes the planet's classical orbital elements.

The optimization problem consists of finding the minimum time trajectory that transfers the E-sail from the initial orbit to the asteroid's heliocentric orbit, for a given value of the sail characteristic acceleration $a_\oplus$. This amounts to maximizing the objective function $J \triangleq -\Delta t_{\mathrm{EA}}$, where Δt_{EA} is the flight time of the first phase. Using an indirect approach (Betts 1998), the optimal thrust direction $\hat{\boldsymbol{a}}$ and the switching parameter τ are obtained by means of Pontryagin's maximum principle, that is, by maximizing at any time the Hamiltonian of the system and taking into account the constraints $\|\hat{\boldsymbol{a}}\| = 1$ and $\alpha \leq \alpha_{\max}$. In particular, the Hamiltonian function of our problem is

$$H \triangleq a_\oplus\,\tau\,\left(\frac{r_\oplus}{r}\right)\,\mathbb{A}\,\hat{\boldsymbol{a}} \cdot \boldsymbol{\lambda} + \boldsymbol{d} \cdot \boldsymbol{\lambda} \tag{22}$$

where $\boldsymbol{\lambda} \in \mathbb{R}^{6\times 1}$ is the adjoint vector

$$\boldsymbol{\lambda} \triangleq [\lambda_p,\, \lambda_f,\, \lambda_g,\, \lambda_h,\, \lambda_k,\, \lambda_L]^{\mathrm{T}} \tag{23}$$

whose time derivative is given by the Euler-Lagrange equations (Bryson and Ho 1975)

$$\dot{\boldsymbol{\lambda}} = -\frac{\partial H}{\partial \boldsymbol{x}} \tag{24}$$

The explicit expressions of the Euler-Lagrange equations, together with the optimal values of the controls $\hat{\boldsymbol{a}}$ and τ as a function of both the state vector and the adjoint vector, have been evaluated using a symbolic math toolbox and are omitted here for the sake of brevity. However, an in-depth discussion of the optimal control law can be found in Quarta and Mengali (2010).

The optimal control problem is mathematically described by the six equations of motion (6) and the six Euler-Lagrange equations (24). This differential system must be completed with 12 suitable boundary conditions. For example, in an optimal orbit-to-orbit transfer, in which both the initial and the final true longitude L are outputs of the optimization process, the first 10 boundary conditions are the values of p, f, g, h, and k on the (Keplerian) heliocentric orbit of both the Earth (at the initial time $t = 0$) and the asteroid 1998 KY26 (at the final time $t = \Delta t_{\mathrm{EA}}$), see Table 1 and Eqs. (15)–(19). The remaining two boundary conditions, together with the constraint necessary to calculate the minimum flight time Δt_{EA}, are obtained by enforcing the transversality conditions (Bryson and Ho 1975; Casalino et al. 1998; Casalino et al. 1999), viz.

$$\lambda_L(t = 0) = 0 \qquad , \qquad \lambda_L(t = \Delta t_{\mathrm{EA}}) = 0 \qquad , \qquad H(t = \Delta t_{\mathrm{EA}}) = 1 \tag{25}$$

where the Hamiltonian function is given by Eq. (22). Note that conditions (25) are necessary but not sufficient for a global optimality of the transfer.

In a rendezvous constrained optimal transfer, twelve boundary conditions are the values of the six MEOE on the (Keplerian) heliocentric orbit of both the Earth (at the initial time) and the asteroid 1998 KY26 (at the final time). In this case, the actual value of the true longitude L on the (Keplerian) heliocentric orbit of the two celestial bodies has been evaluated using a two-body dynamics (that is, without orbital perturbations). In other terms, in this simplified mathematical model, the MEOE p, f, g, h, and k are constants of motion. The minimum flight time is obtained by enforcing the transversality condition that coincides, again, with the last of Eqs. (25).

The simulation results have been obtained by integrating the equations of motion (6), and the Euler-Lagrange equations (24) in double precision using a variable order Adams-Bashforth-Moulton solver scheme (Shampine and Reichelt 1997), with absolute and relative errors of 10^{-12}. The two-point boundary-value problem associated to the variational problem has been solved through a hybrid numerical technique that combines genetic algorithms (to obtain a first estimate of adjoint variables), with gradient-based and direct methods to refine the solution (Mengali and Quarta 2005).

References

Baker, J. (2006). "The falcon has landed." *Science*, 312(5778), 1327. doi: 10.1126/science.312.5778.1327.

Barucci, M., Dotto, E., and Levasseur-Regourd, A. (2011). "Space missions to small bodies: asteroids and cometary nuclei." *Astronomy and Astrophysics Review*, 19(1), 1–29. doi: 10.1007/s00159-011-0048-2.

Betts, J. T. (1998). "Survey of numerical methods for trajectory optimization." *Journal of Guidance, Control, and Dynamics*, 21(2), 193–207.

Betts, J. T. (2000). "Very low-thrust trajectory optimization using a direct SQP method." *Journal of Computational and Applied Mathematics*, 120(1), 27–40.

Bryson, A. E. and Ho, Y. C. (1975). *Applied Optimal Control*. Hemisphere Publishing Corporation, New York, NY, Chapter 2, 71–89.

Casalino, L., Colasurdo, G., and Pastrone, D. (1998). "Optimization procedure for preliminary design of opposition-class Mars missions." *Journal of Guidance, Control, and Dynamics*, 21(1), 134–140. doi: 10.2514/2.4209.

Casalino, L., Colasurdo, G., and Pastrone, D. (1999). "Optimal low-thrust escape trajectories using gravity assist." *Journal of Guidance, Control, and Dynamics*, 22(5), 637–642. doi: 10.2514/2.4451.

Janhunen, P. (2009). "Increased electric sail thrust through removal of trapped shielding electrons by orbit chaotisation due to spacecraft body." *Annales Geophysicae*, 27, 3089–3100. doi: 10.5194/angeo-27-3089-2009.

Janhunen, P. (2010). "Electric sail for producing spacecraft propulsion, <`http://www.patentlens.net/patentlens/patent/US_7641151/`>. Filed March 2, 2006.

Janhunen, P., Mengali, G., and Quarta, A. A. (2007). "Electric sail propulsion modeling and mission analysis." 30th International Electric Propulsion Conference, Florence, Italy (September 17–20). Paper IEPC-2007-352.

Janhunen, P., Toivanen, P. K., Polkko, J., Merikallio, S., Salminen, P., Haeggstrom, E., Seppanen, H., Kurppa, R., Ukkonen, J., Kiprich, S., Thornell, G., Kratz, H., Richter, L., Kromer, O., Roste, R., Noorma, M., Envall, J., Latt, S., Mengali, G., Quarta, A. A., Koivisto, H., Tarvainen, O., Kalvas, T., Kauppinen, J., Nuottajarvi, A., and Obraztsov, A. (2010). "Electric solar wind sail: Towards test missions." *Review of Scientific Instruments*, 81(11), 111301–1–111301–11. doi: 10.1063/1.3514548.

Lewis, J. S. (1996.). *Mining the Sky: Untold Riches from the Asteroid, Comets, and Planets*. Addison-Wesley ISBN: 0-201-32819-4.

Mengali, G. and Quarta, A. A. (2005). "Optimal three-dimensional interplanetary rendezvous using nonideal solar sail." *Journal of Guidance, Control, and Dynamics*, 28(1), 173–177.

Mengali, G. and Quarta, A. A. (2009). "Rapid solar sail rendezvous missions to asteroid 99942 Apophis." *Journal of Spacecraft and Rockets*, 46(1), 134–140. doi: 10.2514/1.37141.

Mengali, G., Quarta, A. A., and Janhunen, P. (2008). "Electric sail performance analysis." *Journal of Spacecraft and Rockets*, 45(1), 122–129. doi: 10.2514/1.31769.

Metzger, P. T., Muscatello, A., Mueller, R. P., and Mantovani, J. (2012). "Affordable, rapid bootstrapping of space industry and Solar System civilization." *Journal of Aerospace Engineering*. doi: 10.1061/(ASCE)AS.1943-5525.0000236 In press.

Ostro, S., Pravec, P., Benner, L., Hudson, R. S., Sarounova, L., Hicks, M. D., Rabinowitz, D. L., Scotti, J. V., Tholen, D. J., Wolf, M., Jurgens, R. F., Thomas, M. L., Giorgini, J. D., Chodas, P. W., Yeomans, D. K., Rose, R., Frye, R., Rosema, K. D., Winkler, R., and Slade, M. A. (1999). “Radar and optical observations of asteroid 1998 KY26.” *Science*, 285(5427), 557–559. doi: 10.1126/science.285.5427.557.

Quarta, A. A. and Mengali, G. (2010). “Electric sail missions to potentially hazardous asteroids.” *Acta Astronautica*, 66(9-10), 1506–1519. doi: 10.1016/j.actaastro.2009.11.021.

Shampine, L. F. and Reichelt, M. W. (1997). “The MATLAB ODE suite.” *SIAM Journal on Scientific Computing*, 18(1), 1–22. doi: 10.1137/S1064827594276424.

Standish, E. M. (1990). “The observational basis for JPL's DE200, the planetary ephemerides of the astronomical almanac.” *Astronomy and Astrophysics*, 233(1), 252–271.

Standish, E. M. (1998). “JPL planetary and lunar ephemerides, DE405/LE405.” *Interoffice Memoradum IOM 312.F-98-048*, Jet Propulsion Laboratory (August 26). Available online (cited May 23, 2012) `http://iau-comm4.jpl.nasa.gov/de405iom/de405iom.pdf`.

Walker, M. J. (1986). “Erratum - a set of modified equinoctial orbit elements.” *Celestial Mechanics*, 38, 391–392.

Walker, M. J. H., Owens, J., and Ireland, B. (1985). “A set of modified equinoctial orbit elements.” *Celestial Mechanics*, 36, 409–419.

List of Tables

List of Figures

orbital element	Earth+Moon barycenter	asteroid 1998 KY26
semimajor axis [AU]	9.99996×10^{-1}	1.23199
eccentricity	1.66928×10^{-2}	2.01378×10^{-1}
inclination [deg]	1.66709×10^{-3}	1.48113
long. of asc. node [deg]	176.223	84.4464
arg. of per. [deg]	286.744	209.182
mean anomaly [deg]	356.926	306.675

Table 1. Reference orbital elements at $\mathrm{MJD} = 55927$ **(January 1, 2012).**

$a_\oplus$ [mm/s^2]	Δt_{AE} [days]	ν_i [deg]	ν_f [deg]	revs.	$a_\oplus^{(ss)}$ [mm/s^2]
1	94.36	189.45	84.11	0	1.0883
0.9	97.85	188.24	85.87	0	1.0430
0.8	102.12	186.76	87.99	0	0.9937
0.7	107.44	184.92	90.59	0	0.94
0.6	118.92	181.49	96.39	0	0.8471
0.5	146.75	172.96	108.76	0	0.7009
0.4	200.91	156.65	129.55	0	0.5604
0.3	371.33	105.75	177.94	0	0.4578
0.2	568.89	170.42	110.35	1	0.2616
0.15	892.26	231.16	105.71	2	0.2161
0.14	929	205.72	105.32	2	0.2163
0.13	973.67	179.71	110.33	2	0.2159
0.12	1040.4	146.62	124.23	2	0.21
0.11	1211.3	106.24	176.75	2	0.1471
0.1	1347.9	204.23	106.98	3	0.1444
0.09	1449.8	152.32	122.22	3	0.1425

Table 2. Orbit-to-orbit optimal performance for Earth-asteroid transfer phase.

$a_\oplus$ [mm/s^2]	Δt_{EA} [days]	ν_i [deg]	ν_f [deg]	revs.	$a_\oplus^{(ss)}$ [mm/s^2]
1	80.46	280.12	184.46	0	1.1003
0.9	83.27	278.91	185.74	0	1.0671
0.8	86.67	277.46	187.27	0	1.03
0.7	92.32	274.79	189.41	0	0.9751
0.6	112.42	265.34	196.05	0	0.8288
0.5	144.76	251.18	206.14	0	0.6879
0.4	205.56	227.74	223.86	0	0.5581
0.3	389.42	176.22	278.05	0	0.4335
0.2	573.67	247.43	211.1	1	0.2597
0.15	897.04	253.89	153.15	2	0.1862
0.14	934.24	253.31	177.76	2	0.1754
0.13	980.46	247.57	203.78	2	0.1649
0.12	1052.49	232.71	238.94	2	0.1541
0.11	1257.63	170.37	283.47	2	0.1395
0.1	1355	251.63	180.87	3	0.1245
0.09	1463.94	234.42	234.16	3	0.1143

Table 3. Orbit-to-orbit optimal performance for asteroid-Earth transfer phase.

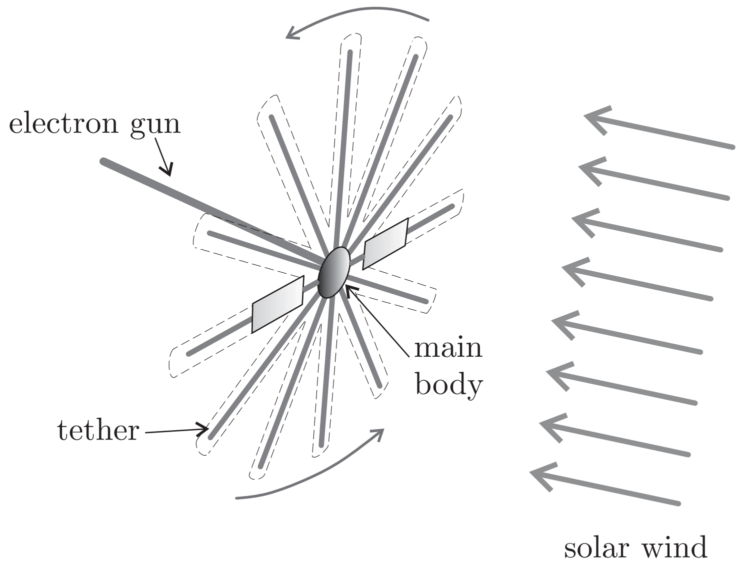

Figure 1. Schematic view of E-sail concept.

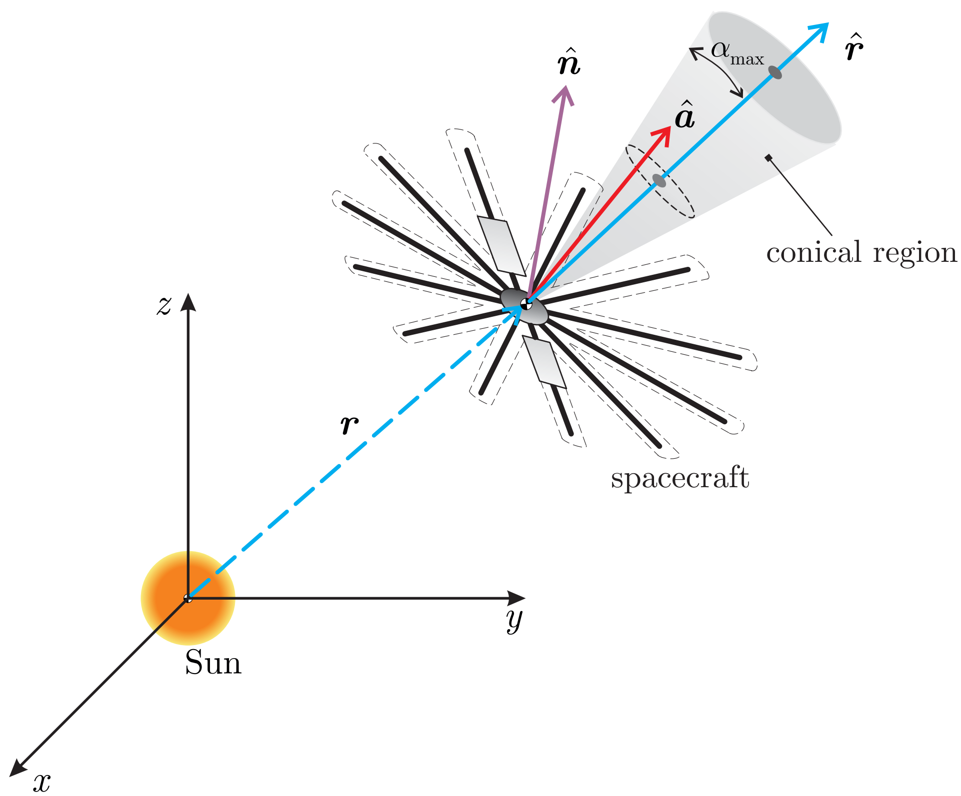

Figure 2. Spacecraft propulsive thrust vector direction.

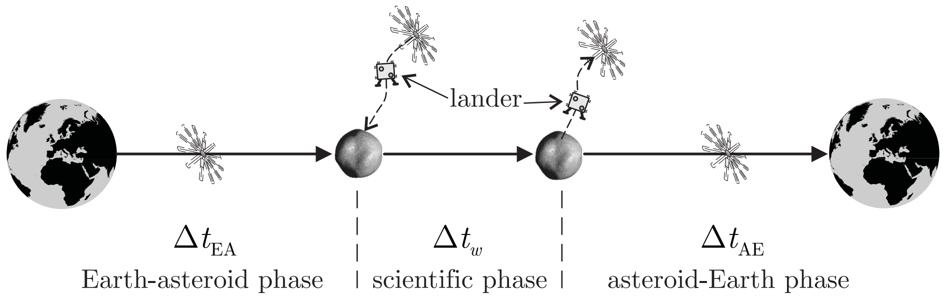

Figure 3. Schematic view of mission phases.

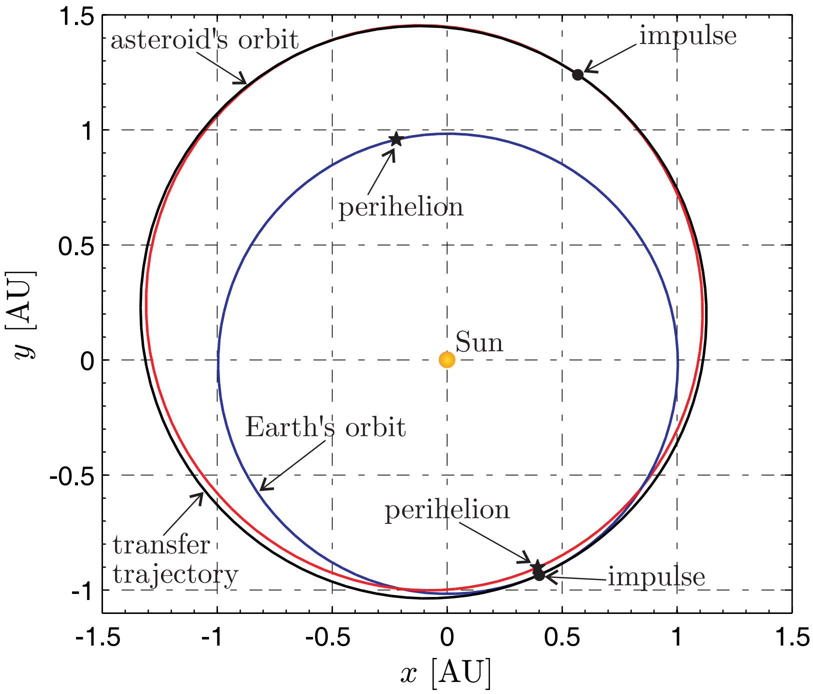

Figure 4. Two-impulse transfer trajectory with minimum velocity variation (orbit-to-orbit transfer).

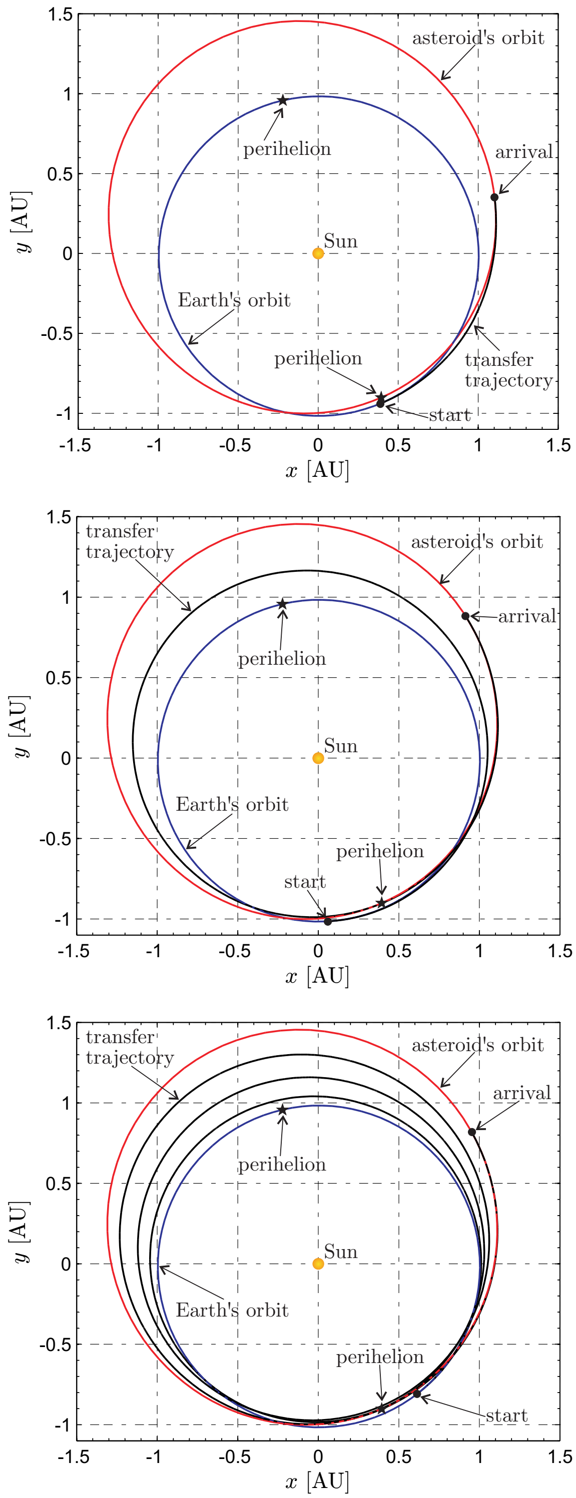

Figure 5. Ecliptic projection of the (orbit-to-orbit) optimal Earth-asteroid transfer trajectory for $a_\oplus = 1$ mm/s^2 (top), $a_\oplus = 0.2$ mm/s^2 (middle), $a_\oplus = 0.1$ mm/s^2 (bottom).

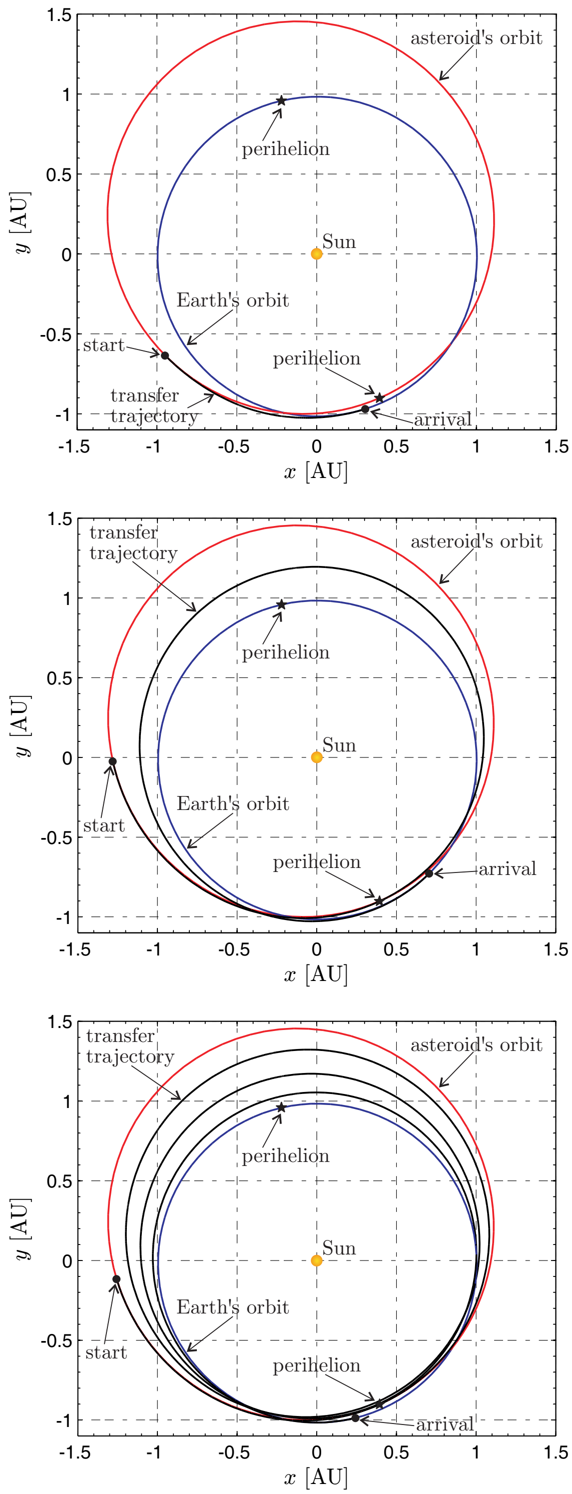

Figure 6. Ecliptic projection of the (orbit-to-orbit) optimal asteroid-Earth transfer trajectory for $a_\oplus = 1$ mm/s^2 (top), $a_\oplus = 0.2$ mm/s^2 (middle), $a_\oplus = 0.1$ mm/s^2 (bottom).

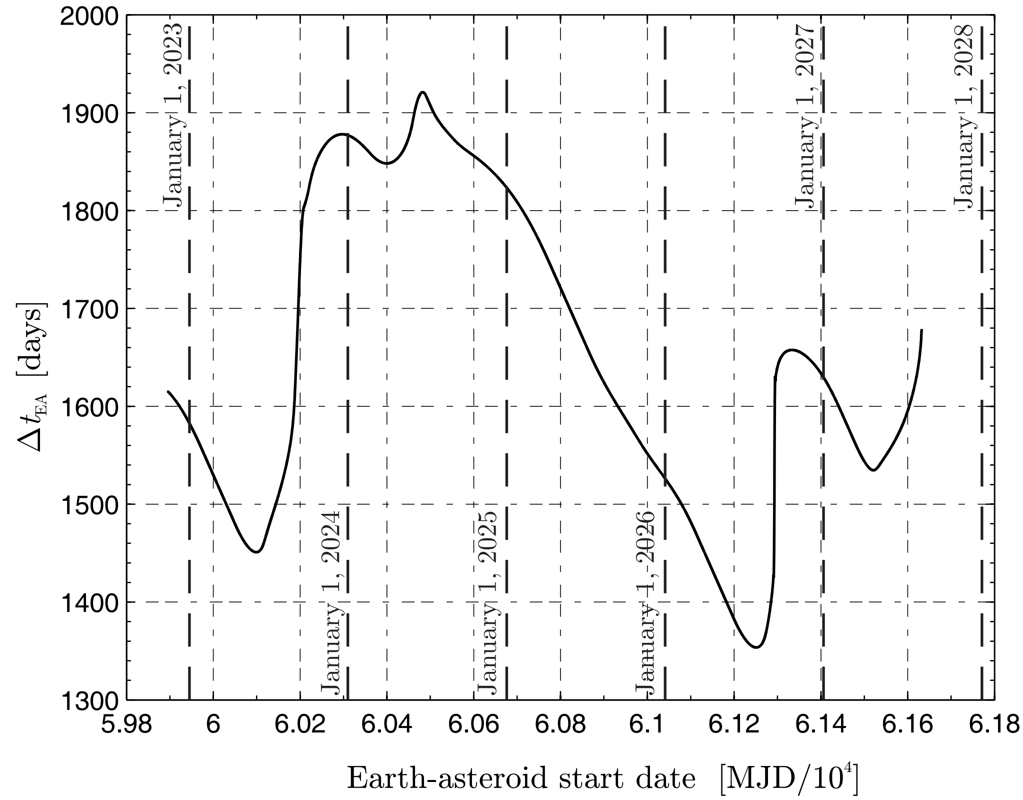

Figure 7. Earth-asteroid minimum transfer time as a function of the Modified Julian Date for $a_{\oplus} = 0.1$ mm/s^2.

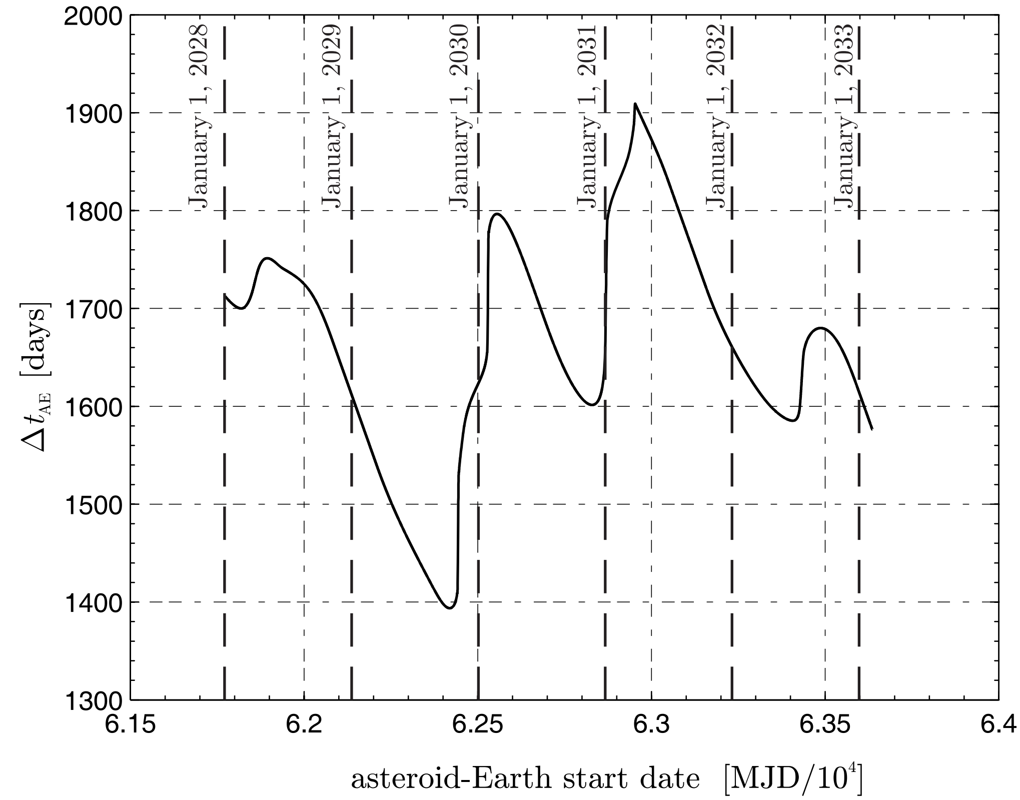

Figure 8. Asteroid-Earth minimum transfer time as a function of the Modified Julian Date for $a_\oplus = 0.1$ mm/s^2.

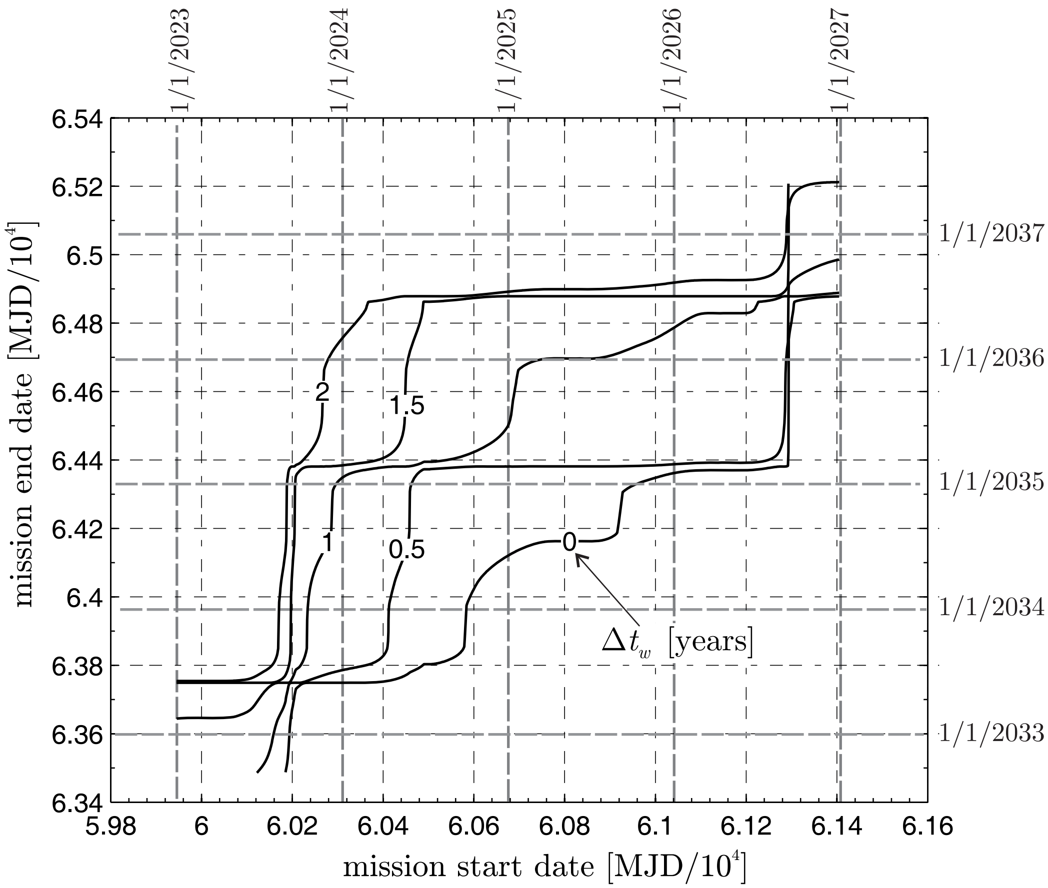

Figure 9. Mission end date as a function of waiting time Δt_w and start date ($a_\oplus = 0.1$ mm/s^2).